

Electronic Supplementary Material (ESI) for Journal of Materials Chemistry C.
This journal is © The Royal Society of Chemistry 2016

Supporting Information

Revealing the Influence of Solvent Evaporation Rate and Thermal Annealing on Molecular Packing and Charge Transport for DPP(TBFu)₂

*Guangchao Han,^{ab} Xingxing Shen,^{ab} Ruihong Duan,^{ab} Hua Geng,^a Yuanping Yi^{*a}*

^aBeijing National Laboratory for Molecular Sciences, CAS Key Laboratory of Organic
Solids, Institute of Chemistry, Chinese Academy of Sciences, Beijing 100190, China

^bUniversity of Chinese Academy Sciences, Beijing 100049, China

*Corresponding author. E-mail: ypyi@iccas.ac.cn

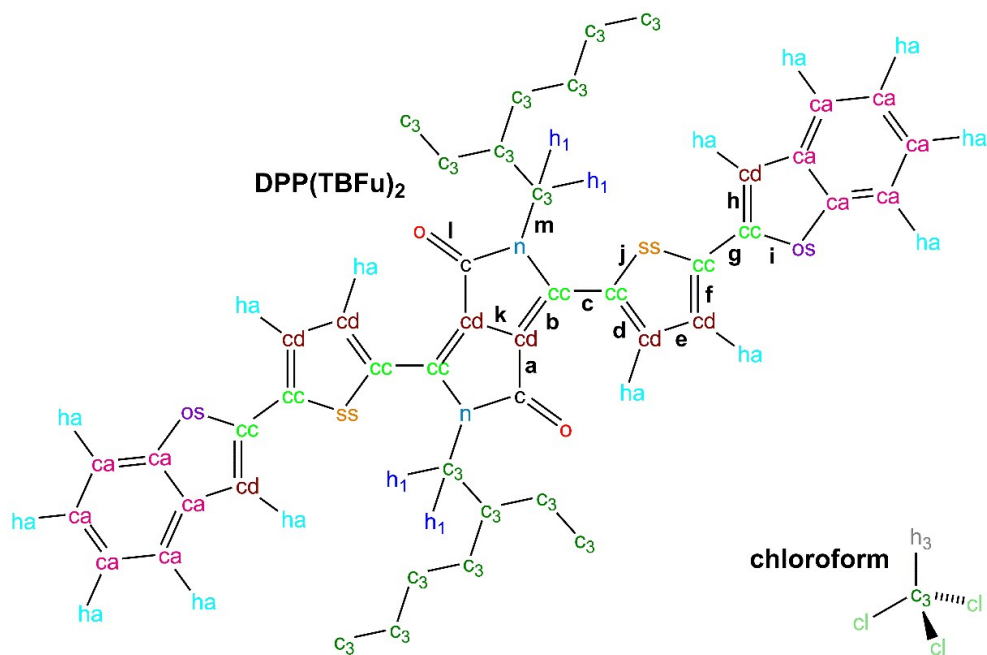


Figure S1. Atomic type definitions for DPP(TBFu)₂ and chloroform from the general AMBER force field (GAFF). The hydrogen atoms connected to the c3 are defined as hc.

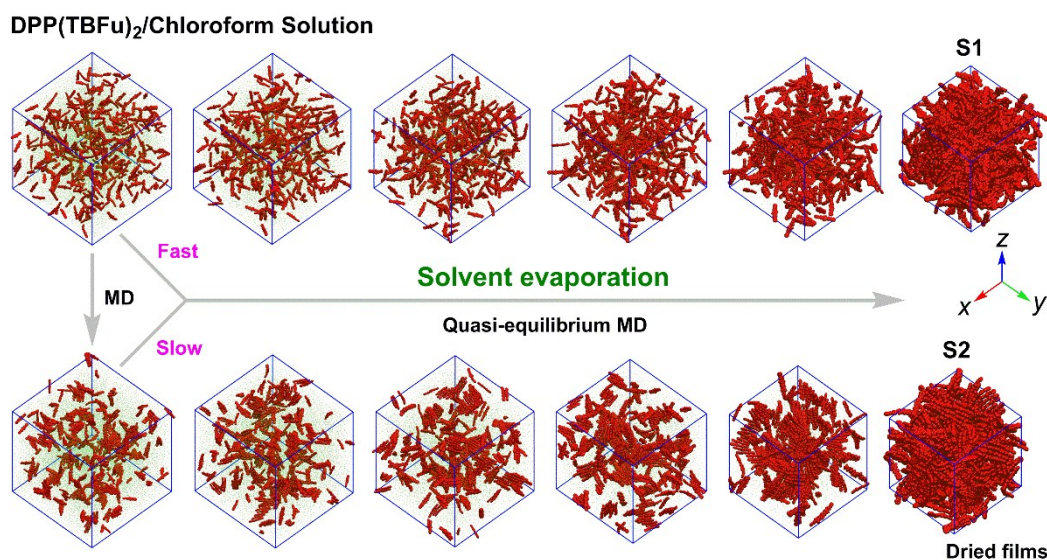


Figure S2. Construction of a DPP(TBFu)₂/chloroform solution and simulations of the supramolecular self-assemblies of DPP(TBFu)₂ during solvent evaporation. The inherent alkyl chains of DPP(TBFu)₂ and hydrogen atoms are neglected for visualizing the packing of conjugated backbones, and the chloroform molecules are simplified as points with the carbon atoms' positions. DPP(TBFu)₂ backbones and chloroform points are colored in red and green, respectively. The dried films obtained with relatively fast and slow evaporation rate are labeled as **A1** and **B1**.

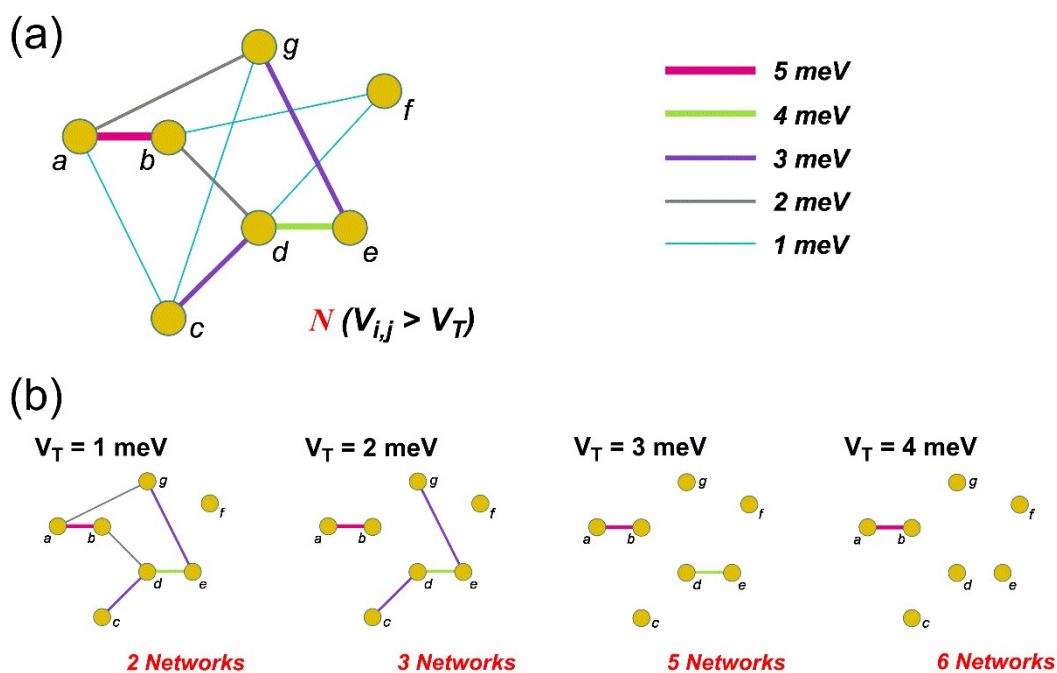


Figure S3. (a) An example graph of vertices (a-g) and edges (lines), in which the vertices represent the center-of-masses of molecules and the edge thickness corresponds to the strength of electronic coupling between molecules. (b) Returned networks with a variable electronic coupling threshold.

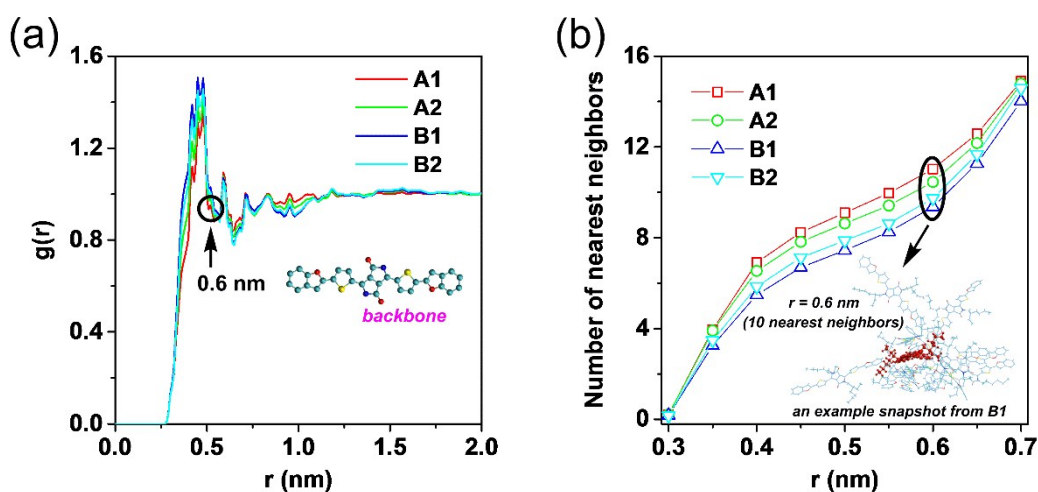


Figure S4. (a) Backbone radial distribution functions (RDFs) of four well-fabricated DPP(TBFu)₂ samples. (b) Number of nearest neighbors as a function of shortest interatomic distance between backbones. Note that 0.6 nm corresponds to the first valley in the backbone RDFs.

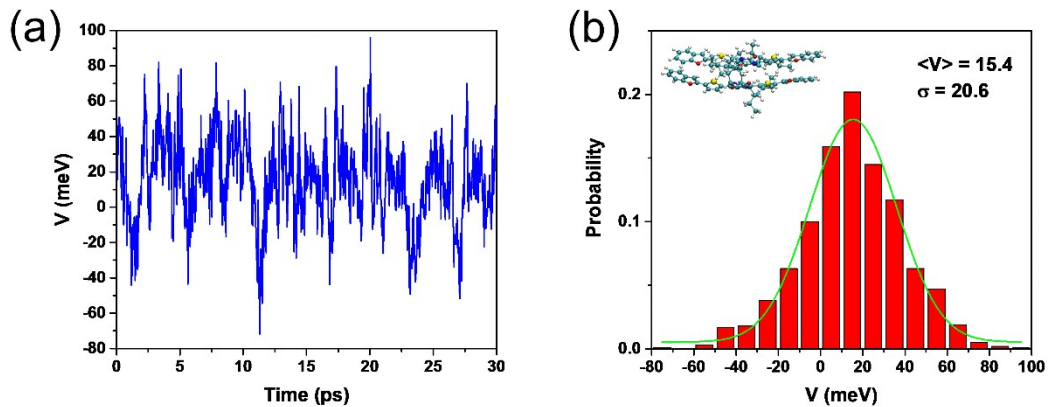


Figure S5. (a) Fluctuation of the transfer integrals for holes as a function of time for a selected dimer. (b) Gaussian fitting of the dispersion of transfer integrals (green line).

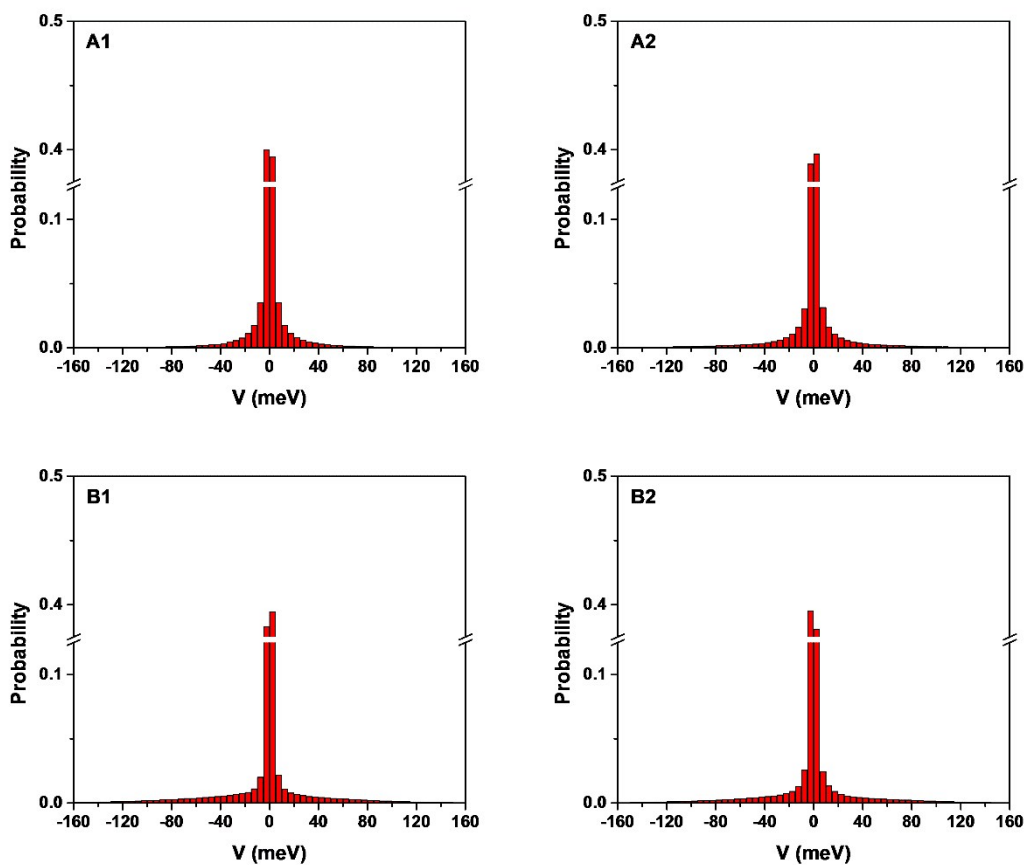


Figure S6. Probability distributions of the transfer integrals for each sample.

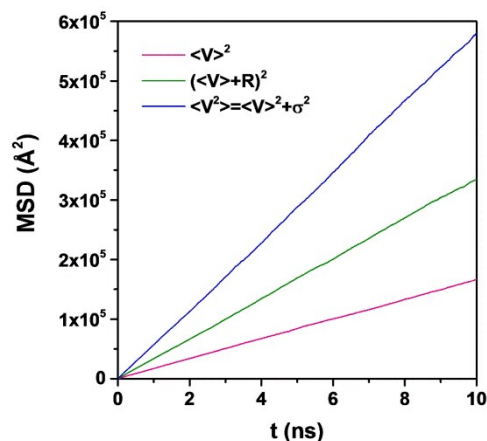


Figure S7. The mean square displacement versus diffusion time for A1 obtained by averaging 5000 kinetic Monte Carlo simulations. Note that three forms of the square of the transfer integral were used to evaluate the diffusion coefficient.

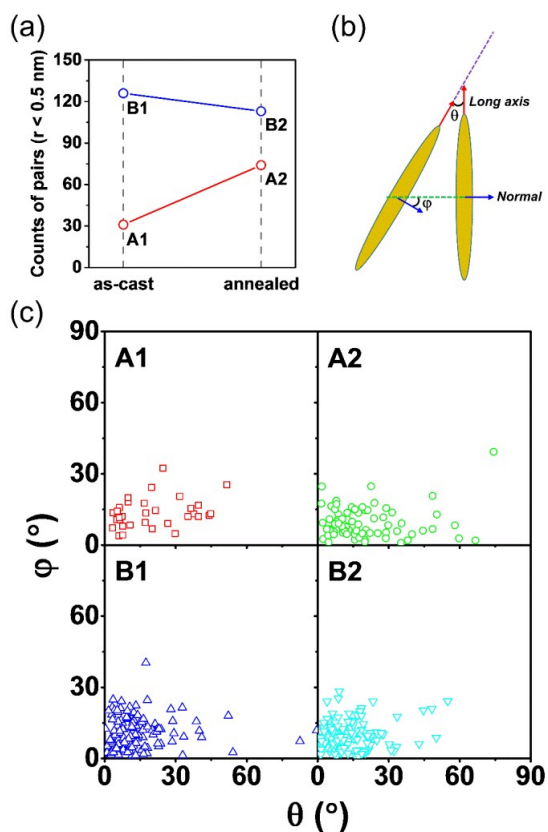


Figure S8. (a) Counts of molecular pairs for each sample. Two molecules with the distance between DPP center-of-masses < 0.5 nm are defined as a molecular pair. (b) Scheme of intermolecular orientation described by two angles: θ , the angle between the long axes, and φ , the angle between the normals of DPP face. (c) A representative snapshot of orientational distributions of molecular pairs for each sample.

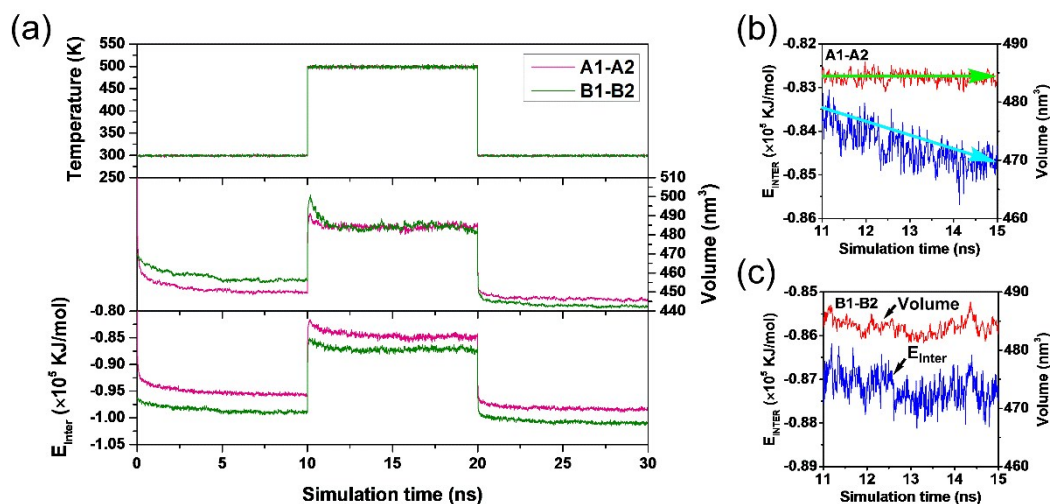


Figure S9. (a) Temperature, volume, and intermolecular interaction energy (E_{INTER}) as a function of simulation time after solvent evaporation (0-10 ns: equilibration at 300 K, 10-20 ns: thermal annealing at 500 K, 20-30 ns: re-equilibration at 300 K; the volume of the fresh dried sample [corresponding to 0 ns] is larger for A1 [524.6 nm³] than B1 [470.0 nm³]). (b, c) Volume and E_{INTER} of A1 (b) and B1 (c) during annealing time of 11-15 ns.

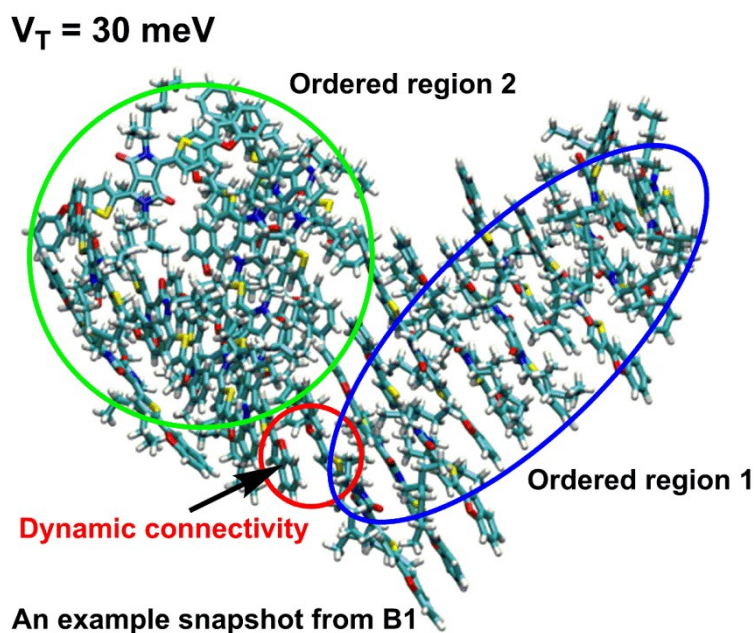


Figure S10. Two relatively ordered regions from B1 with $V_T = 30 \text{ meV}$.

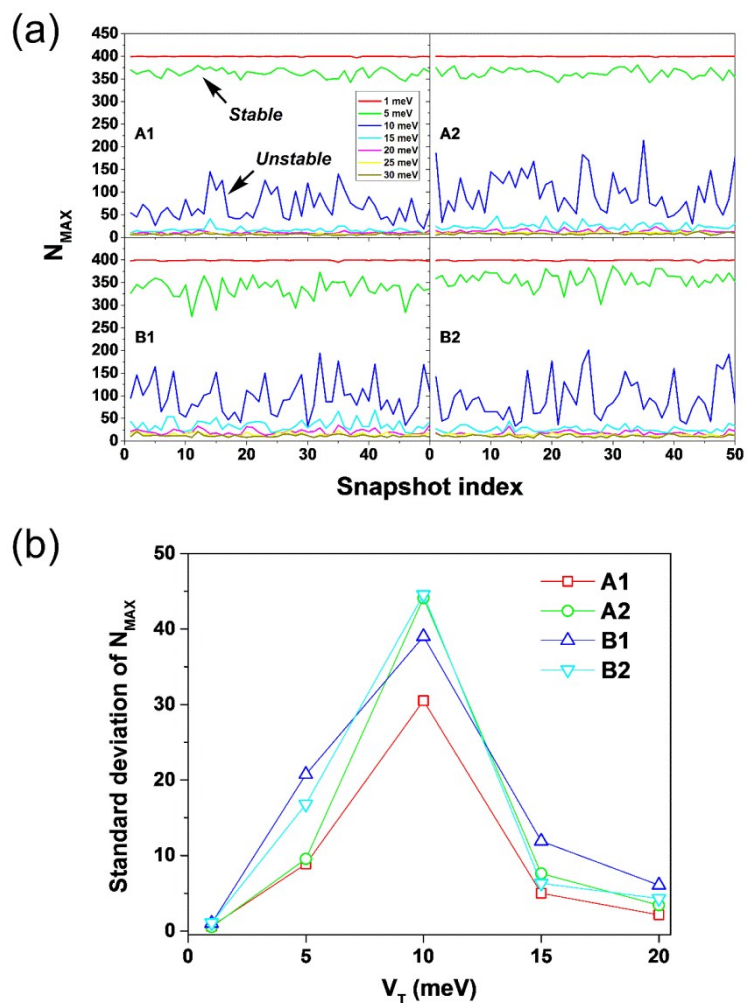


Figure S11. (a) The number of molecules (N_{MAX}) of the largest network for each sample with coupling threshold (V_T) from 1 to 30 meV as a function of snapshots. Snapshots were sampled at 10 ps intervals. (b) Standard deviation of average N_{MAX} for each sample with V_T from 1 to 20 meV.

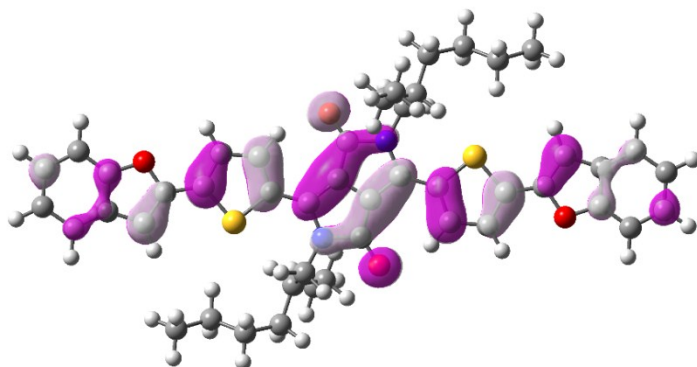


Figure S12. HOMO orbital of DPP(TBFu)₂ calculated at the level of B3LYP/6-31G**.

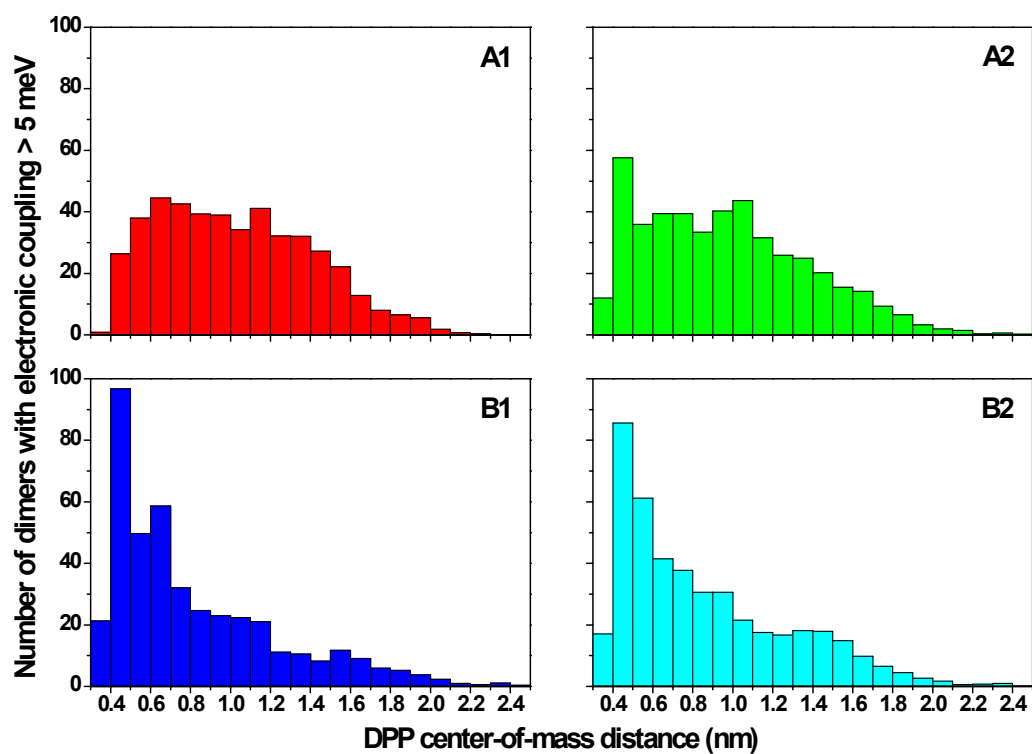


Figure S13. Number of dimers with electronic coupling more than 5 meV as a function of DPP center-of-mass distance for each sample.

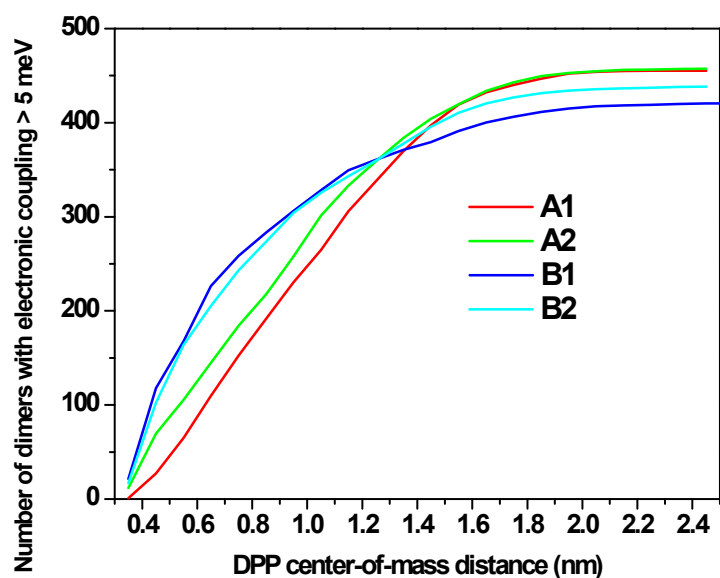


Figure S14. Cumulative number of dimers with electronic coupling more than 5 meV as a function of DPP center-of-mass distance for each sample.

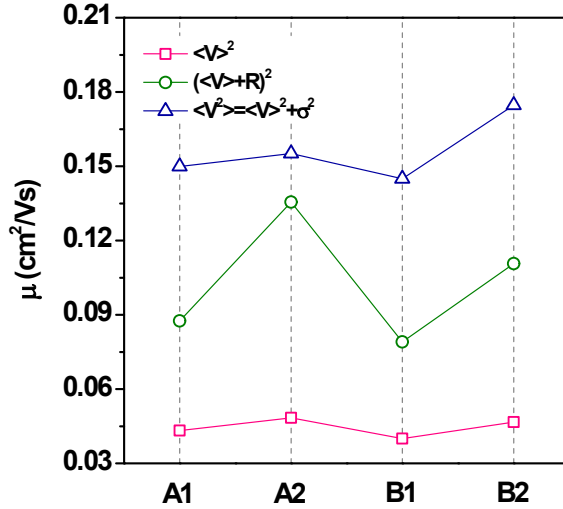


Figure S15. Calculated hole mobilities for each sample according to the MLJ formula.

Considering the non-negligible quantum nature of the most active modes governing local electronic-phonon coupling, the charge transfer rates between DPP(TBFu)₂ molecules to evaluate the hole mobility were also computed according to the Marcus-Levich-Jortner (MLJ) quantum correction of the Marcus equation:¹

$$k_{ij} = \frac{V_{ij}^2}{\hbar} \sqrt{\frac{\pi}{\lambda_{class} k_B T}} \times \sum_{\nu=0}^{\infty} \left[\exp(-S_{eff}) \frac{S_{eff}^{\nu}}{\nu!} \times \exp\left(-\frac{(\Delta G_{ij} + \lambda_{class} + \nu \hbar \omega_{eff})^2}{4\lambda_{class} k_B T}\right) \right] \quad (S1)$$

where λ_{class} is the classical contribution to the reorganization energy and the quantum description of nonclassical degrees of freedom represented by a single effective mode of frequency ω_{eff} and corresponding Huang-Rhys (HR) factor S_{eff} , which can be determined as:

$$\omega_{eff} = \sum_m \omega_m \frac{S_m}{\sum_n S_n} \quad (S2)$$

and the HR factor S_{eff} follows from the relation $\lambda_i = \hbar \omega_{eff} S_{eff}$, λ_i is the intramolecular reorganization energy. The HR factors were obtained through the DUSHIN program developed by Reimers.² The contributions for frequencies below 250 cm⁻¹ were not included in the evaluation of ω_{eff} , which were summed to the λ_{class} . The outer reorganization was assumed to be 0.001 eV, also included in λ_{class} . The estimated values of λ_{class} , S_{eff} , and ω_{eff} are 0.023 eV, 2.187, and 984.932 cm⁻¹, respectively. Using the procedure described in Computational Methods, the hole mobilities based on the MLJ formula were calculated, shown in **Figure S15**.

Table S1. Comparison of selected bond lengths (**Figure S1**) calculated for an isolated DPP(TBFu)₂ molecule via two computational methods (GAFF and B3LYP/6-31G**) and the X-ray crystallographic geometry.³

	a	b	c	d	e	f	g	h	i	j	k	l	m
GAFF	1.45	1.39	1.46	1.38	1.43	1.37	1.43	1.38	1.39	1.75	1.40	1.21	1.48
B3LY	1.44	1.40	1.44	1.39	1.41	1.38	1.44	1.37	1.38	1.76	1.42	1.23	1.46
P													
Exp.	1.45	1.38	1.44	1.39	1.41	1.37	1.44	1.34	1.39	1.74	1.41	1.23	1.46

Table S2. Lattice parameters of a DPP(TBFu)₂ (5×14×3) supercell obtained from the NPT simulations with GAFF compared to experiment.³

	Exp. (100 K)	Simulation (100 K)	Simulation (300 K)
a	14.181	14.272 (+0.64%)	14.722
b	5.165	5.193 (+0.54%)	5.243
c	26.304	25.939 (-1.39%)	26.332
α	90.000	90.000 (0.00%)	89.980
β	91.393	90.590 (-0.88%)	87.820
γ	90.000	90.000 (0.00%)	89.900

REFERENCES

- 1 J. Jortner, *J. Chem. Phys.*, 1976, **64**, 4860-4867.
- 2 J. R. Reimers, *J. Chem. Phys.*, 2001, **115**, 9103-9109.
- 3 J. Liu, Y. Zhang, H. Phan, A. Sharenko, P. Moonsin, B. Walker, V. Promarak, T.-Q. Nguyen, *Adv. Mater.*, 2013, **25**, 3645-3650.